Numerical Optimization of Hybrid Dielectric/HTS Resonators for Surface Impedance Evaluation of HTS Films

C. Collado, D. Gonzalo, E. Rozan, J.M. O'Callaghan.
Universitat Politècnica de Catalunya. Campus Nord UPC-D3. Barcelona 08034, Spain.

C. Sans
Universitat de Vic. C/ Miramarges 4. Vic 08500, Spain

Abstract— This work describes an alternative to the traditional dielectric resonator topology used for measuring surface impedance in High Temperature Superconducting (HTS) films. A gap is introduced above the dielectric so that only the lower film is in direct contact with it. This arrangement has been used extensively for mechanical tuning of dielectric resonators and, when used for surface impedance measurement, it can be designed to make the losses in the upper film small relative to the overall resonator losses. Then, measured results are mostly due to one of the films and not the average of two. The specifics of a resonator design for measuring 2-inch wafers are presented. An analysis and optimization of the resonator is done using a numerically efficient mode-matching algorithm.

I. INTRODUCTION

Commonly used techniques for evaluating surface impedance in HTS thin films are based on measurements of resonators on either patterned, planar structures or in a dielectric resonator cavity in which the upper and lower walls are made of HTS films and are in contact with the dielectric [1]. Only the latter approach is non-destructive, but it yields the average surface resistance of two films. Thus, to measure a sample with unknown properties, it has to be paired with a reference sample to determine its surface impedance. The degree of accuracy to which the surface resistance of the reference is known can be a significant source of error in these measurements. Therefore, other non-destructive methods need to be explored further.

II. HYBRID DIELECTRIC/HTS RESONATOR

The dielectric resonator topology under study is a modification of the traditional dielectric-HTS one [1], where a gap is introduced between the upper endplate and the dielectric cylinder (Fig. 1). The purpose of introducing this gap is to lower the RF losses in the upper film and
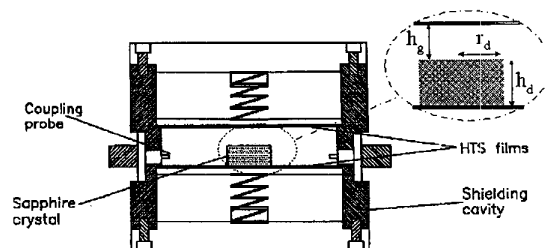
Fig. 1. Dielectric resonator structure. Definitions of dielectric height (h_d), dielectric radius (r_d) and gap size (h_g)

concentrate them in the lower one, so that its R_s is the largest contributing factor to the total losses of the cavity.

Experimental use of this type of cavity for measurement of R_s is mentioned in [2], but no design details are given. An analytical study of this topology, based on an axial mode-matching method with a single mode is presented in [3]. No description is given in any of these works of the procedure to optimize the cavity for R_s determination purposes. In [3] it is pointed out that, as the upper gap is increased, the electromagnetic fields on the normal metal side walls also increase, so the contribution of the RF losses of the upper film are reduced at the expense of increasing those of the side walls. For R_s determination, an optimal height exists for a given resonator size and a given diameter of the superconducting endplates, for which the ratio of the RF losses in the lower plate to the overall losses in the cavity is maximum. This optimum may be found using an efficient mode-matching code [4], which calculates the electromagnetic field distribution in structures with azimutal symmetry. The algorithm is not restricted to small gap sizes and can be used to optimize the whole structure (gap size, dielectric height and dielectric diameter) for a given diameter of the supeconducting wafers to be measured.

Reference [2] proposes a surface resistance determination procedure based in two consecutive measurements of quality factors in which the top and bottom samples are exchanged. The optimization proposed here might make this unnecessary, so that a single measurement and a rough estimate of the surface resistance of the top film and side walls might lead to an accurate determination of the surface resistance of the lower film.
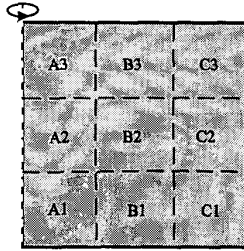
Fig. 2. Radial regions (A,B,C) and axial layers (1,2,3) considered by the mode-matching algorithm. Dielectric permitivity can be defined independently for each of the 9 cells (A1..C3).

A. Full-wave radial mode-matching method

The software developed [4] can analyze up to three different radial regions, each one divided into three different layers (Fig.2). The dielectric constant in each region and layer can be set independently, and the whole volume analyzed is assumed to be enclosed by conducting walls. Fields in every radial region are expressed as an infinite series of particular solutions of the wave equation in cylindrical coordinates.

Azimutal and axial eigenfunctions are harmonic functions while radial eigenfunctions are Bessel functions, which must be chosen appropriately to avoid singularity in the axis (region A), fulfill boundary conditions on the external walls (region C), or provide continuity between adjacent regions (region B). The eigenvalues of each radial region are found by solving a pair of transcendental equations related to the three-layer problem. A system of equations is then found by forcing continuity conditions of the tangential fields between radial regions A and B, and B and C, from which the coefficients of the mode expansion are found. In our case 12 modes are sufficient. Fig. 3 illustrates the field and current distributions for a sapphire dielectric with a 12 mm diameter and a 6 mm height.

B. Optimization. Basics and alternatives

For R_s determination, the optimal dimensions of the cavity in Fig. 1 are those that make the losses of the lower plate dominant with respect to the other type of losses. This is equivalent to maximizing Q_0/Q_{low}, where:

$$Q_0 = \frac{\omega_0 U}{P_d}; \quad Q_{low} = \frac{\omega_0 U}{P_{d\_low}}, \quad (1)$$

U is the total stored energy in the cavity, P_d the total dissipated power, P_{d_low} the power dissipated in the lower wall, and Q_0 the unloaded quality factor. Both the total energy U and the dissipated powers P_d and P_{d_low} can be calculated from the field distribution inside the cavity with properly defined surface and volume integrals of the electromagnetic fields [5]. Definitions analogous to that of Q_{low} in (1) can be used for Q_{up}, Q_{sd} and Q_d which account for the losses in the upper wall, side wall, and dielectric respectively. Thus, the unloaded quality factor can be written as:
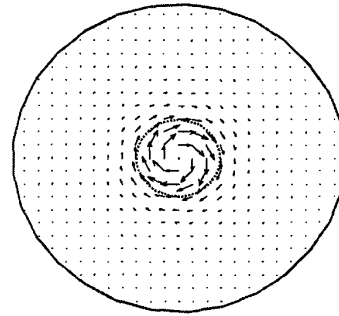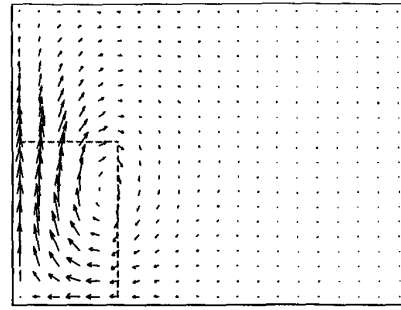

Fig. 3. Field and current distributions in the cavity with a TE$_{01}$ mode and a sapphire dielectric. Bottom plate diameter is 48mm, dielectric diameter is 12mm and dielectric height is 6mm. The dashed line represents the sapphire outline. (Top) Radial cut of the resonator showing magnetic field lines. (Bottom) Currents at the surface of the lower HTS film.

$$\frac{1}{Q_0} = \frac{1}{Q_{low}} + \frac{1}{Q_{up}} + \frac{1}{Q_{sd}} + \frac{1}{Q_d}. \quad (2)$$

The relevance of maximizing Q_0/Q_{low} is due to the fact that this defines the sensitivity of the system:

$$\left| \frac{\Delta Q_0/Q_0}{\Delta R_s/R_s} \right| = \frac{Q_0}{Q_{low}}, \quad (3)$$

which can. be proven from (1) and (2), and from the proportionality between P_{d_low} and R_s. Also, as Q_0/Q_{low} is increased, the accuracy in estimating Q_{up}, Q_{sd} and Q_d has a lesser effect on the R_s predicted from the measured Q_0 and (2).

A software code has been developed, which includes the electromagnetic mode-matching algorithm described previously, and is capable of calculating Q_{low}, Q_{up}, Q_{sd} and Q_d as a function of dielectric height (h_d), dielectric radius (r_d) and gap size (h_g) (Fig. 1). To test it, the cavity dimensions given in [2] were used, and the code results were compared with those in Table I in that reference. The agreement is excellent, as shown in Table I of this work.

The software developed can use several strategies to vary h_d, r_d and h_g in the search for a maximum of Q_0/Q_{low} : 1) variation of the gap size for a given (fixed) dimension of the dielectric; 2) exhaustive search varying h_d, r_d and h_g over a specified range, with a specified incremental step size; and 3)

TABLE I
COMPARISONS BETWEEN [2] AND THIS WORK

Glow is defined as the product of the surface resistance of the lower plate and *Qlow*; *Gup* and *Gsd* are defined similarly.

	f (GHz)	Glow	Gup	Gsd
[2]	9.5	546	4.90e3	1.15e6
This work	9.510	541	4.81e3	1.11e6
Error %		0.8%	1.7%	3.3%

gradient search using *Matlab* [6]. In this process it is assumed that the upper and lower walls are made of $YBa_2Cu_3O_{7-\delta}$ (YBCO), and the side walls of a normal metal (usually OFHC copper, but it can be changed by the user). Their R_s is scaled as the calculated resonant frequency of the cavity changes due to variations in h_d, r_d and h_g. The scaling law is taken as f^2 for YBCO and $f^{1/2}$ for the metal, and the values of R_s at 10GHz and 77K are taken as $300\mu\Omega$ (YBCO) and $9m\Omega$ (Cu) [7] respectively. The frequency dependence of the loss tangent of sapphire is neglected, taking $\tan\delta = 4\ 10^{-8}$ [8] throughout the optimization.

C. Optimum gap for fixed dielectric and wafer sizes

When dimensions of the wafer and the dielectric are known and fixed, only h_g needs to be varied to find a maximum for Q_0/Q_{low}. This is done for two reasons: to explore a possible improved design of the cavity in [2] (while maintaining the sapphire used); and to find a good initial set of values of h_d, r_d and h_g from which a second optimization can be done using a gradient search in which all three variables are allowed to change.
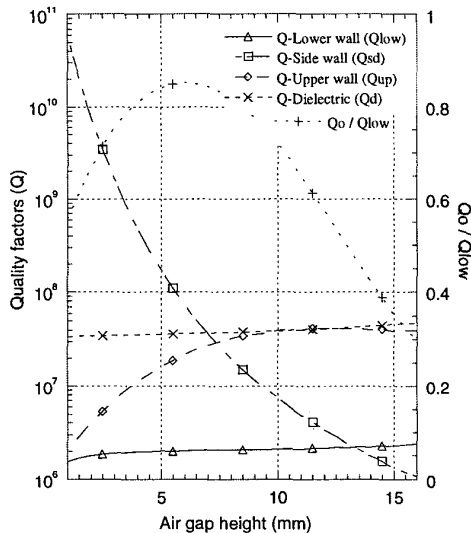
Fig. 4 shows the results of the gap height optimization for a dielectric with h_d=6mm, r_d=6mm and a 2 inch wafer where only an area of 48mm in diameter is exposed to the electromagnetic fields in the cavity. This figure indicates that, while the losses in the side walls are strongly dependent on h_g, this dependence is moderate in the upper wall, and weak in the dielectric and lower wall. Therefore, the optimum height represents a trade-off between the losses in the upper wall and those in the side wall. This results in an optimum gap of h_g=6mm and Q_0/Q_{low}=0.85, which essentially coincides with the results reported in [2]. As shown later, substantial improvements can be made by adjusting h_d, r_d and h_g jointly.

Finally, Fig. 5 shows that these results degrade strongly if the diameter of metal side wall is reduced.

D. Substitution of the upper HTS plate by a cooper one

Unsuccessful attempts have been made at replacing the YBCO in the upper wall by copper. Even when the gap height optimization process was performed taking into account the new R_s of the upper plate, the sensitivity (Q_0/Q_{low}) values were too low to allow an acceptable accuracy in the determination of the R_s of the bottom plate. In other words, the gap can never be high enough to replace the upper film by a normal metal without making it a dominant source of loss in the cavity and rendering it useless for surface resistance determination. Fig. 6 shows the effects of this substitution in the sensitivity (Q_0/Q_{low}).

E. Joint optimization of h_d, r_d and h_g

The values of h_d, r_d and h_g have been optimized using two parallel approaches: a gradient optimization and an

Fig. 4. Dependence of Q_{up}, Q_{low}, Q_{sd} with gap height (h_g). The optimum height (max. Q_0 /Q_{low}) represents a trade-off between the losses in the upper and side walls (Q_{up}, Q_{sd}), whose dependence on h_g is much stronger than that of the lower wall (Q_{low}) and dielectric (Q_d). The maximum of Q_0/Q_{low} is at h_g=6mm.
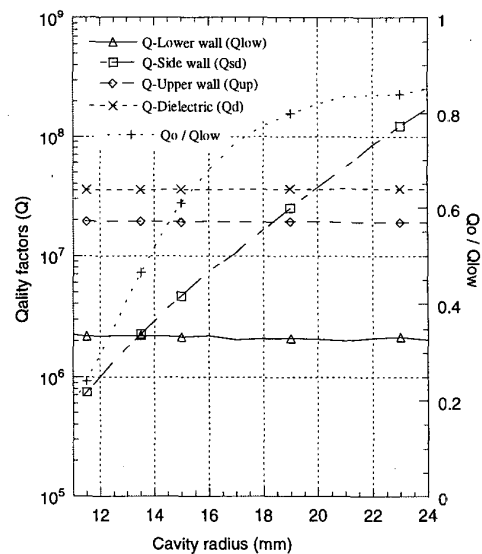
Fig. 5. Dependence of Q_{up}, Q_{low}, Q_{sd} with cavity radius. As the radius is decreased, losses in the side walls increase, become dominant, and degrade Q_0 /Q_{low}. Gap height is h_g=6mm. As in Fig. 4, dielectric height is h_d=6mm
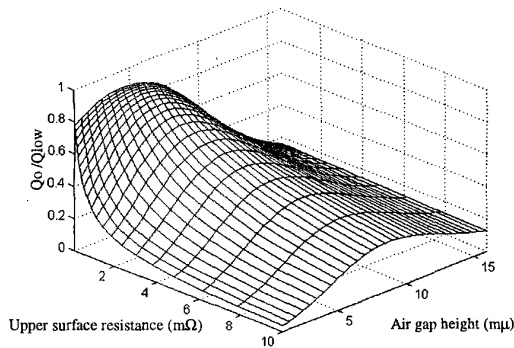
considered in a cavity with these dimensions, only a 5%
overestimation of the surface resistance of the lower sample
will be made, and this may be greatly with estimates of the
surface resistance of the side walls, upper film and dielectric
loss tangent.

III. CONCLUSION

An optimization of the image dielectric resonator cavity
has been done by numerical techniques. The software
developed for the optimization has been cross-checked with
previously published results. The optimized cavity should be
allow the determination of surface resistance of YBCO with
an error lower than 5% if no other sources of RF loss in the
cavity are taken into account.

Fig. 6. Deterioration of the sensitivity (Q_0/Q_{low}) as the value of R_s of the
upper sample is increased. A strong degradation occurs for the range of
R_s values corresponding to cooper at 77K at the resonant frequencies of
the cavity (about 10 mΩ). For these values of R_s in the upper wall, the
Q_0/Q_{low} is too low for determination of the R_s of the lower HTS film.

exhaustive search over a broad range of h_d, r_d and h_g to ensure
that the gradient optimization did not stop at a local
maximum of Q_0/Q_{low}.

The exhaustive search was done from 2mm< h_d<10mm,
3mm<r_d<14mm and 1mm<h_g<15mm. A maximum was found
at h_d=2mm, r_d=5mm and h_g=6mm with Q_0/Q_{low}=0.94. The
search showed that this optimum value would degrade sharply
when h_d was decreased beyond its optimum value. However,
the dependence with h_d and r_d was much weaker.

Gradient optimizations were run starting from several
values, including the ones from Sect. II-C. They all reached
similar values of Q_0/Q_{low}. The best one was the one started
from h_d=2mm, r_d=5mm and h_g=6mm (the optimum of the
exhaustive search), which was used to fine-tune the previous
search resulting in h_d=1.7mm, r_d=5.0mm and h_g=4.6mm with
Q_0/Q_{low} =0.95. In other words, if no other losses are

REFERENCES

[1] Z-Y Shen, C. Wilker, P. Pang, W. L. Holstein, D. Face, D.J. Konutz. "High Tc Superconductor-Sapphire Microwave Resonator with Extremely High Q-Values up to 90K". *IEEE Trans. Microwave Theory Tech.*, vol. 40 no. 12, pp 2424-2432. Dec. 1992.

[2] C. Zuccaro, N. Klein, A. G. Zaitsev, R. Wördenweber, Y. Lemaitre, and J.C. Mage. "Nonlinear microwave losses of large area YBCO thin films. *Applied Superconductivity 1997*, Inst. Phys. Conf. Ser. no 158, pp 295-298 [Proceedings EUCAS 1997].

[3] N. Tellman, N. Klein, U. Dähnem, H. Schulz, and H. Chaloupka. "High Q LaALO₃ dielectric resonator shielded by YBCO films". *IEEE Trans. Appl. Superconduct.*, vol 4, no. 3, pp143-148, Sept. 1994.

[4] Sans, J.M. O'Callaghan, D. Sancho, R. Pous, J. Fontcuberta, J.-F. Liang and G.C. Liang. "Full-wave analysis of the image hybrid dielectric/HTS resonator". *IEEE Trans. Appl. Superconduct.*, vol 4, no. 7, pp3840-3844, Dec. 1997.

[5] R.F. Harrington. *Time-Harmonic Electromagnetic Fields*. McGraw-Hill, 1961.

[6] The Mathworks, Inc. *Matlab user's guide*.

[7] G.W.C. Kaye and T.H. Laby. *Table of physical and Chemical constants*. Longmans Green London, 1966.

[8] Z.-Y. Shen. *High Temperature Superconducting Microwave Circuits*. Artech House, 1994.